Chinese Journal of
POLYMER SCIENCE

ARTICLE

https://doi.org/10.1007/s10118-018-2106-y
Chinese J. Polym. Sci. 2018, 36, 888–896

Self-assembly Behavior of Symmetrical Linear ABCA Tetrablock Copolymer: A Self-consistent Field Theory Study

Dan Liu[a], Ying-Ying Wang[b,c], Ying-Chun Sun[a*], Yuan-Yuan Han[a], Jie Cui[b*], and Wei Jiang[b]

[a] *School of Physics, Northeast Normal University, Changchun 130024, China*
[b] *State Key Laboratory of Polymer Physics and Chemistry, Changchun Institute of Applied Chemistry, Chinese Academy of Sciences, Changchun 130022, China*
[c] *University of Chinese Academy of Sciences, Beijing 100049, China*

Abstract ABCA tetrablock copolymers offer new opportunities for design of materials with novel structures. Using real-space self-consistent field theory and simulation, we systematically examined the self-assembly behavior of linear ABCA tetrablock copolymers in a 2D space. The simulation was carried out under conditions of symmetrical compositions and interactions. We focus on the influence of chain length ratio of block A and interactions between block A and other blocks B and C on the self-assembly behavior of the copolymer system. The simulation results show that most of the structures self-assembled by the ABCA tetrablock copolymers are centrosymmetric, such as diblock-like lamella phase, two kinds of lamellae with beads at interface, two kinds of hierarchical lamella phase, hexagonal honeycomb-like phase, lamella phase with mixed BC and hexagonal spheres with mixed BC. Furthermore, we find that a novel noncentrosymmetric Janus spheres can be obtained when the interaction between blocks B and C is strong, whereas a noncentrosymmetric lamella phase was obtained at weak interaction between blocks B and C. Phase diagrams for the ABCA tetrablock copolymers with different interaction strength between blocks B and C are constructed by comparing free energies of candidate ordered structures. In addition, studies on the metastable behavior of the system reveal that enthalpy plays an important role in the metastable behavior of the ABCA tetrablock copolymer system. Our work can provide useful guide for structure control of such kind of tetrablock copolymers in experiments.

Keywords Self-assembly; Tetrablock copolymer; Self-consistent field; Simulation

Citation: Liu, D.; Wang, Y. Y.; Sun, Y. C.; Han, Y. Y.; Cui, J.; Jiang, W. Self-assembly Behavior of Symmetrical Linear ABCA Tetrablock Copolymer: A Self-consistent Field Theory Study. Chinese J. Polym. Sci. 2018, 36(7), 888–896.

INTRODUCTION

Block copolymers (BCPs), constructed by linking chemically dissimilar linear chains together, can spontaneously self-assemble into various exquisitely ordered structures at nanoscale, which have great potentials in applications such as metamaterials[1, 2], membranes[3], nanowire[4] and lithography[5–7]. As the simplest BCPs, linear AB diblock copolymers can self-assemble into the well-known structures including body-centered cubic spheres, hexagonally packed cylinders, bicontinuous gyroids and parallel lamellae[8, 9]. New structure generally implies new functions and properties. To extend the available variety of structures, more chemically distinct blocks are linked together to form more complicated block copolymers, *e.g.*, linear and star ABC triblock copolymers. The self-assembly behavior of these copolymers has been extensively explored to date, both by experiments and computer simulations[10–21]. Many fascinating periodic structures that cannot be obtained in AB diblock copolymers have been obtained in ABC triblock copolymers.

In principle, increasing the number of blocks and the block types can markedly increase the number of accessible nanostructures self-assembled by block copolymers[22]. However, great challenges in structure searching and control also emerge due to the rapid expansion of the parameter space with the increase in the number of blocks and block types[23]. For instance, the simplest linear AB diblock copolymers can be modeled using only two parameters (*i.e.*, 2D parameter space), that is $\chi_{AB}N$ and f_A (where χ_{AB} is the Flory-Huggins interaction parameter, N the chain length and f_A the chain length ratio of block A). When it comes to ABC triblock copolymers, at least five parameters (*i.e.*, 5D parameter space formed by $\chi_{AB}N$, $\chi_{BC}N$, $\chi_{AC}N$, f_A and f_B) should be considered to describe their phase behavior. If the number of blocks and block types are further increased, the parameter space will be vastly expanded to such an extent that no existing research means (experimental and computational) can bear. Therefore, on one hand, people expect to acquire more complicated block copolymers by increasing the number of blocks and block types. On the other hand, great expansion in parameter space is expected to

* Corresponding authors: E-mail sunyc149@nenu.edu.cn (Y.C.S.)
E-mail jcui@ciac.ac.cn (J.C.)

Received September 18, 2017; Accepted December 26, 2017; Published online February 27, 2018

be avoided. In this context, people are now paying more and more attentions to linear ABCA tetrablock copolymers[23–29]. Compared with the existing ABC triblock copolymers, the introduction of a fourth block into the ABC triblock copolymer does not increase the block types, hence does not excessively expand the parameter space. Meanwhile, it provides an extra control parameter, which can offer unique opportunities for materials design. In addition, people also found that the ABCA tetrablock copolymers can be used to obtain materials with asymmetric structures[30, 31]. For example, using poly(isoprene-block-styrene-block-isoprene-block-2-vinylpyridine) (PI-PS-P2VP-PI) tetrablock copolymer, Takano *et al*. obtained a kind of polymeric materials with noncentrosymmetric lamellae, which has potentials in applications such as nonlinear optics[30]. Theoretically, this kind of noncentrosymmetric lamellae were later studied by Jaffer *et al*[31]. In addition, Brannan *et al*. and Cui *et al*. respectively studied the self-assembly behavior of the ABCA tetrablock copolymers in solution by experiment and simulation. They all obtained asymmetric vesicles that have different inner and outer hydrophobic layers, which can be used to mimic cell membranes to control drug loading and release[25, 26, 32]. In the past decade, continuous efforts were also devoted to the synthetic techniques to synthesize various ABCA tetrablock copolymers[27–29]. As the corresponding study gradually deepens, a comprehensive understanding about the self-assembly behavior of the ABCA tetrablock copolymers appears to be more necessary for fabrications of materials with desirable structures. Up to now, however, there have been very few studies on the self-assembly behavior of the ABCA tetrablock copolymers. Only a few discrete points in the parameter space have been considered. The effects of the interaction parameters between different blocks, as well as the chain length ratio, on the self-assembly behavior of the ABCA tetrablock copolymers remain unclear. Aiming at this situation, we studied the self-assembly behavior of the ABCA tetrablock copolymers in this work using computer simulation method, because compared with experiments, computer simulations are more suitable for structure exploration and prediction with a relatively low time and economic consumption.

In this work, the self-consistent field theory (SCFT) was employed. The SCFT is one of the most widely used methods in the study of phase behavior of polymers, and the SCFT has proven to be a powerful tool to explore complex structures formed by block copolymers[10, 11, 13, 15, 33–35]. Using the SCFT and simulation, we systematically studied the self-assembly behavior of linear ABCA tetrablock copolymers in a 2D space. The calculation was performed respectively at weak and strong interactions between middle blocks B and C. We focused our work on the influence of the interactions between end blocks A and middle blocks B and C, as well as the chain length ratio of block A, on the self-assembly behaviors of the systems. Various structures were obtained in our simulations. Phase diagrams comprehensively showing the variations of the self-assembly structures with the chain length ratio of block A and the interaction strength between middle blocks B and C were provided to offer more insight into the phase behavior of the ABCA tetrablock copolymer.

MODEL AND METHOD

In this section, we briefly introduce the SCFT method. We consider an incompressible linear ABCA tetrablock copolymer with chain length N in a rectangular 2D lattice. The chain length ratios of segments A, B and C in the block copolymer are f_A, f_B, f_C and $f_A + f_B + f_C = 1$. In this work, the block lengths of the two end blocks A are set equal (their chain length ratios are $f_A/2$, respectively), and the two middle blocks B and C also have equal chain length ratios (*i.e.*, $f_B = f_C$), as shown in Fig. 1.

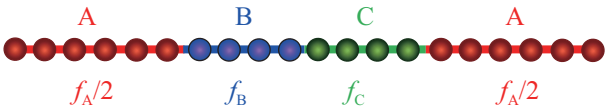

Fig. 1 Schematic of the linear ABCA tetrablock copolymer (The two end blocks A have equal chain length ratios of $f_A/2$. The chain length ratios of the two middle blocks B and C are equal, *i.e.*, $f_B = f_C$. The blocks A, B and C are represented by red, blue and green, respectively.)

For the block copolymer system we consider, the free energy (in unit of k_BT) is given by

$$F = -\ln(Q/V) - 1/V\int d\vec{r}\cdot\left[\sum_\alpha \omega_\alpha(\vec{r})\phi_\alpha(\vec{r}) + P(\vec{r})(1-\sum_\alpha \phi_\alpha(\vec{r}))\right] + 1/(2V)\int d\vec{r}\cdot\left[\sum_{\alpha\neq\beta}\chi_{\alpha\beta}N\phi_\alpha(\vec{r})\phi_\beta(\vec{r})\right] \quad (1)$$

where $\chi_{\alpha\beta}$ is the Flory-Huggins interaction parameters between species α and β(α, β = A, B and C), and $\phi_\alpha(\vec{r})$ is the density fields of species α. $P(\vec{r})$ is the Lagrange multiplier that enforces the incompressibility. $Q = \int d\vec{r}\cdot q(\vec{r},1)$ is the partition function of a single polymer chain in effective conjugated chemical potential fields $\omega_A(\vec{r})$, $\omega_B(\vec{r})$ and $\omega_C(\vec{r})$. $q(\vec{r},s)$ is the end-segment distribution function that gives the probability of finding segment s at position $\vec{r}$. The contour variable s is parameterized so that it changes continuously from 0 to 1, corresponding to moving from one end of the chain to the other end along the chain contour. The end-segment distribution function satisfies the modified diffusion equation.

$$\frac{\partial q(\vec{r},s)}{\partial s} = \begin{cases} \nabla^2 q(\vec{r},s) - \omega_A(\vec{r},s)q(\vec{r},s) & (0 \le s \le f_A/2) \\ \nabla^2 q(\vec{r},s) - \omega_B(\vec{r},s)q(\vec{r},s) & (f_A/2 < s \le f_A/2+f_B) \\ \nabla^2 q(\vec{r},s) - \omega_C(\vec{r},s)q(\vec{r},s) & (f_A/2+f_B < s \le f_A/2+f_B+f_C) \\ \nabla^2 q(\vec{r},s) - \omega_A(\vec{r},s)q(\vec{r},s) & (f_A/2+f_B+f_C < s \le 1) \end{cases} \quad (2)$$

https://doi.org/10.1007/s10118-018-2106-y

Eq. (2) satisfies the initial condition $q(\vec{r},0)=1$. A second end-segment distribution function $q^+(\vec{r},s)$ is also needed in this work. $q^+(\vec{r},s)$ also satisfies Eq. (2) but with the right-hand side multiplied by -1 and with the initial condition of $q^+(\vec{r},1)=1$. The density field of each component can be obtained by

$$\phi_A(\vec{r})=\frac{V}{Q}[\int_0^{\frac{f_A}{2}} ds\cdot q(\vec{r},s)q^+(\vec{r},s) + \int_{\frac{f_A}{2}+f_B+f_C}^{1} ds\cdot q(\vec{r},s)q^+(\vec{r},s)] \quad (3)$$

$$\phi_B(\vec{r})=\frac{V}{Q}\int_{\frac{f_A}{2}}^{\frac{f_A}{2}+f_B} ds\cdot q(\vec{r},s)q^+(\vec{r},s) \quad (4)$$

$$\phi_C(\vec{r})=\frac{V}{Q}\int_{\frac{f_A}{2}+f_B}^{\frac{f_A}{2}+f_B+f_C} ds\cdot q(\vec{r},s)q^+(\vec{r},s) \quad (5)$$

Minimizing the free energy with respect to the density fields and the Lagrange multiplier leads to the following equations:

$$\omega_A(\vec{r})=\chi_{AB}N(\phi_B(\vec{r})-f_B) + \chi_{AC}N(\phi_C(\vec{r})-f_C)+P(\vec{r}) \quad (6)$$

$$\omega_B(\vec{r})=\chi_{AB}N(\phi_A(\vec{r})-f_A) + \chi_{BC}N(\phi_C(\vec{r})-f_C)+P(\vec{r}) \quad (7)$$

$$\omega_C(\vec{r})=\chi_{AC}N(\phi_A(\vec{r})-f_A) + \chi_{BC}N(\phi_B(\vec{r})-f_B)+P(\vec{r}) \quad (8)$$

$$\phi_A(\vec{r})+\phi_B(\vec{r})+\phi_C(\vec{r})=1 \quad (9)$$

Eqs. (3)–(9) form a closed set of self-consistent equations that can be solved self-consistently in the real-space. In this work we employed the algorithm proposed by Drolet and Fredrickson to solve the self-consistent field equations[36, 37]. According to the algorithm adopted by Drolet and Fredrickson, the density fields in Eqs. (6)–(8) are subtracted by their spatial average values[37]. It should be noted that these subtracted terms are imposed, but not obtained by functional derivative of Eq. (1) with respect to the density fields. Using the combinatorial screening algorithm proposed by Drolet and Fredrickson[36, 37], firstly, by randomly generating the initial values of $\omega_\alpha(\vec{r})$, q and q^+ can be obtained by solving the modified diffusion equations using the Crank-Nicholson scheme and an alternating direction implicit (ADI) algorithm[38]. Subsequently, the density fields of each component $\phi_\alpha(\vec{r})$ are calculated based on Eqs. (3)–(5). The Lagrange multiplier $P(\vec{r})$ is obtained by solving Eqs. (6)–(9)[39]. Finally, the chemical potential field $\omega_\alpha(\vec{r})$ can be updated by means of a linear mixing of new and old solutions[37, 39]. After obtaining new chemical fields $\omega_\alpha(\vec{r})$, a new iteration can be performed with the new $\omega_\alpha(\vec{r})$ as initial values. This procedure is iterated until the morphologies are invariable with time and the free energy change is less than 10^{-4}. In this paper, the numerical simulations were carried out in a 2D rectangular lattice with a size of $V=L_x\times L_y$. Periodic boundary conditions were imposed in x- and y- directions. We know that the free energy of the system can be influenced by the lattice size. If the lattice size is incommensurate with the intrinsic period of ordered structure, the system will have higher free energy. Therefore, the lattice size should be finely adjusted to minimize the free energy of ordered structure as possible. In this work, the lattice sizes L_x and L_y are firstly varied from 100 to 120, and the grid size is set to be $dx=dy=0.05R_g$ (R_g is the unperturbed radius of gyration of the linear triblock copolymer chain). By varying the lattice size, a series of candidate ordered structures can be obtained in simulations. After obtaining the candidate structures, the grid size is further varied to minimize the free energy of the ordered structures. Since there are two periods for some structures in this work, we adjusted the lattice size along different directions by varying dx and dy within the range of $(0.05\pm0.003)R_g$, respectively. Structure with the lowest free energy is defined as stable state, whereas other structures with the higher free energies are defined as metastable states. The total chain length of the tetrablock copolymer is fixed at $N=200$.

In addition, it should be noted that simulations performed in 2D space undoubtedly will miss some structures that can only be obtained in 3D space, such as body-centered cubic spheres and bi or tricontinuous gyroid structures. However, this does not mean that 2D simulations are artificial. On one hand, some 3D structures (*e.g.*, lamella and cylinder) that have translational invariance along a certain direction can be investigated by 2D simulations. On the other hand, 2D system can correspond to thin films with thickness comparable to the radius of gyration of polymer chains. In practice, many materials that have great potential applications due to their 2D ordered structures are fabricated in thin film. Therefore, 2D simulations are significant for structure control in experiments.

RESULTS AND DISCUSSION

Firstly, we would like to point out that even with the restrictions of equal chain length ratio of end blocks A and equal chain length ratio of middle blocks B and C, we still have to face a four-dimensional parameter space. A complete exploration in such parameter space is a formidable task. Therefore, the current simulations were carried out under conditions with symmetrical interactions, that is, the interactions between the end blocks A and the other two middle blocks B and C are kept equal by setting $\chi_{AB}N=\chi_{AC}N$. Two values of $\chi_{BC}N$ were selected in this work to represent strong and weak interactions between middle blocks B and C, respectively. Fig. 2 shows all typical structures discovered in our simulations. Regions rich in A, B, C and mixed B and C are exhibited in red, blue, green and grey, respectively. For clarity, all configurations shown in Fig. 2 are constructed by replicating the final pattern 4 times.

Self-assembly Behavior under Strong Interaction between Middle Blocks B and C

In this section, we first studied the self-assembly behavior of

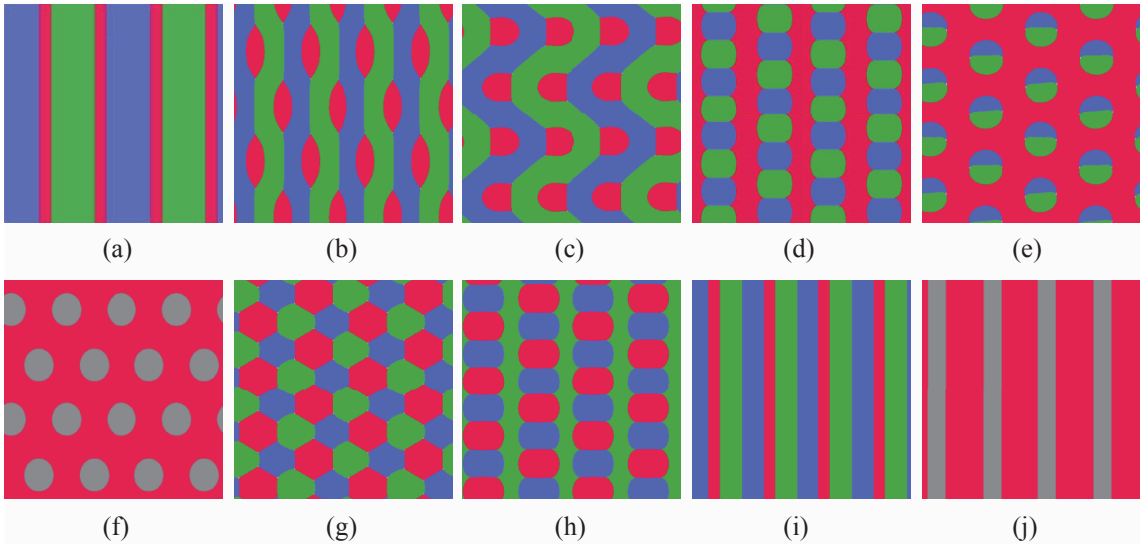

Fig. 2 (a) Diblock-like lamella phase (di-LAM); (b) Lamella phase with beads at interface (LAM+BD-I); (c) Zigzag lamella phase with beads at interface (LAM+BD-II); (d) Hierarchical lamella with continuous A phase (HL-I); (e) Hexagonal Janus phase (HJ); (f) Hexagonal spheres with mixed BC (S-mixBC); (g) Hexagonal honeycomb-like phase (HHL); (h) Hierarchical lamellae with discrete A phase (HL-II); (i) Noncentrosymmetric lamella phase (NCL); (j) Lamella phase with mixed BC (L-mixBC) (Regions rich in A, B, C and mixed B and C are exhibited in red, blue, green and grey, respectively.)

the ABCA tetrablock copolymers when the interaction between middle blocks B and C is strong by setting the interaction parameter $\chi_{BC}N = 50$. Using stable structures obtained at each calculated point, a phase diagram showing the influence of the chain length ratio of block A (f_A) and the interaction parameter between blocks A and B (*i.e.*, $\chi_{AB}N$. Note that $\chi_{AB}N = \chi_{AC}N$) is displayed in Fig. 3. Regions for typical metastable structures are also plotted in Fig. 3, which are discussed in subsequent section. Besides a small disorder region, we can see that most of the area shown in Fig. 3 is occupied by phase-separated region, in which phase separation between different blocks occurs. In the phase-separated region, the phase diagram can be further divided into two parts. One is BC-phase-separated region (denoted by solid symbols), in which blocks B and C phase separate

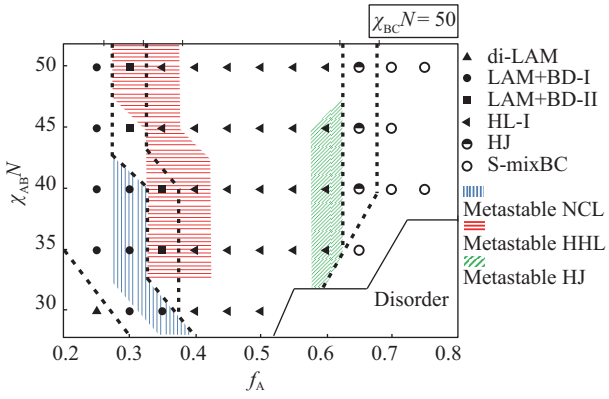

Fig. 3 Phase diagram as a function of chain length ratio of block A f_A and interaction parameter between blocks A and B $\chi_{AB}N$ at $\chi_{BC}N = 50$ (The dashed lines are used to approximately distinguish phase regions for various stable structures. Mesh grids represent regions for typical metastable structures.)

from each other. The other is BC-mixed region, in which blocks B and C are mixed together (denoted by hollow symbols). Our work is mainly focused on the BC-phase-separated region.

Firstly, we note that when the chain length ratio of block A is very small and the interactions between blocks A and the other two blocks B and C are not sufficiently strong, the tetrablock copolymer will tend to reduce into BC-like diblock copolymer. In this case, blocks B and C self-assemble into parallel lamella phase, and most of blocks A are dissolved in domains formed by blocks B and C while only a small amount of blocks A are enriched at interfaces between lamellae (di-LAM phase in Fig. 2a). Since our work is focused on the self-assembly behavior of the tetrablock copolymer, most phase region of di-LAM structure is neglected, and only a very small region can be seen in Fig. 3. From Fig. 3 we can see that when the interaction parameter $\chi_{AB}N$ is higher than 30 and $f_A \approx 0.25$, a narrow phase region representing lamella phase with beads at interface, *i.e.*, LAM + BD-I (Fig. 2b), will be obtained at each value of $\chi_{AB}N$. In this phase, end blocks A self-assemble into discrete bead-like domains due to small chain length ratio, whereas blocks B and C form continuous and straight lamella phase, respectively. Structures similar to LAM+BD-I phase have already been obtained by other researchers in star and linear ABC triblock copolymers[10, 11, 13, 14, 17]. Our simulation result indicates that the same structures can also be obtained in the linear ABCA tetrablock copolymers. Obtaining identical structures from different types of block copolymers is significant for fabrications of materials with similar structures but different properties and performances. In addition, from the Monte Carlo simulations reported by Gemma *et al.*, we can see that star ABC triblock copolymers can form two kinds of 3D structures relating to Fig. 2(b)[17].

https://doi.org/10.1007/s10118-018-2106-y

One is lamella+rod structure, which has translational invariance, hence is identical with the structure shown in Fig. 2(b). The other is lamella+sphere structure. The lamella+sphere structure has no translational invariance but has cross sections that are the same as Fig. 2(b). The same situation can also be seen in linear ABC triblock copolymer system[11]. This indicates that simulations performed in 2D space will miss some structures that do not have translational invariance in 3D space. However, 2D simulations are still valuable and significant for structure control in experiments. This is because 2D system can correspond to thin films with thickness comparable to the radius of gyration of polymer chains, while many materials that have great potential applications are just fabricated in thin film.

When the chain length ratio of block A is increased, another kind of lamella phase with beads at interface, *i.e.*, LAM+BD-II (Fig. 2c) is obtained, and corresponding phase region is on the right side of the LAM+BD-I region, as shown in Fig. 3. Compared with LAM+BD-I phase, in LAM+BD-II phase, the continuous lamella phase domains formed by blocks B and C are no longer straight, but zigzag. As far as we know, structure similar to LAM+BD-II has not been reported in literature.

Subsequently, when the chain length ratio of blocks A is further increased, we find a hierarchical lamellae phase (HL-I in Fig. 2d), the phase region of which occupies the center of the phase diagram. In the HL-I region, the end blocks A self-assemble into continuous and parallel lamellae, whereas middle blocks B and C also form parallel lamellae as a whole. However, in the phase domain formed by blocks B and C, blocks B and C further separate to form B/C alternating domains. It should be noted that similar HL-I phase is a kind of phase generally observed in star ABC triblock copolymer systems, and the formation of HL-I is mainly due to the constraint that A, B and C three blocks are linked together at one junction point[14–17]. However, our simlation results indicate that ABCA teterablcok copolymer, a kind of linear molecule, can also form HL-I phase. Moreover, according to previous studies, the continuous lamella phase in HL-I phase self-assembled by star ABC triblock copolymers is generally formed by the block that has a chain length ratio larger than 50%. However, our simulation results show that the end block A can also form a continuous lamella domain even when its chain length ratio is as low as 40%. On the other hand, similar to the case shown in Fig. 2(b), Fig. 2(d) probably represents more than one kind of 3D structures such as the hierarchical lamellar and the hierarchical cylinder (or called columnar piled disk)[15, 17, 23]. Moreover, we can see from Fig. 3 that the HL-I phase occupies most of the phase-separated regions, meaning that this structure can be obtained in a very wide parameter window in experiment.

Another worth-to-mention simulation result is that a narrow phase region at $\chi_{AB}N \geqslant 40$ and $f_A \approx 0.65$ can be seen in Fig. 3. In this region, the majority blocks A form a matrix, whereas the minority blocks B and C together self-assemble into hexagonally packed spheres. Interestingly, blocks B and C further separate from each other, forming a novel type of structure, *i.e.*, hexagonal Janus phase (HJ phase in Fig. 2e). It should be pointed out that the structure shown in Fig. 2(e) is a kind of noncentrosymmetric structure. The noncentrosymmetric structures are rare in nature. Materials with noncentrosymmetric structure are believed to have special electrical and optical properties. Gemma *et al*. once expected but failed to obtain the HJ phase in star ABC triblock copolymer by means of Monte Carlo simulation[17]. Bates *et al*. also predicted the existence of the HJ phase in ABCA tetrablock copolymers by analyzing the ratio of interfacial surface areas of different phase domains[23]. Our simulation result is in agreement with the prediction of Bates *et al*. In fact, in the parameter space considered in this work, Bates *et al*. also predicted other possible 3D structures that cannot be obtained in 2D space, including axial segregated cylinders, ferromagnetic-like arrangement of Janus spheres. More details about possible 3D structures formed by ABCA tetrablock copolymers can be seen in Ref. [23].

When the chain length ratio of blocks A is increased to an extremely high value, hexagonally packed spheres formed by blocks B and C can still be obtained. However, blocks B and C are mixed homogeneously in this case (S-mixBC in Fig. 2f). Phase separation between blocks B and C does not occur because their chain length ratios are too low.

In the aspect of experiment, Radlauer *et al*. reported a kind of controlled synthesis of ABCA' tetrablock copolymers in a very recent work[29]. They synthesized a series of polystyrene-polyisoprene-polylactide-polystyrene (PS-PI-PLA-PS) tetrablock copolymers with various chain length ratios. They chose three series of the tetrablock copolymers to study their self-assembly morphologies. Some samples (*e.g.*, samples SILS'_E1, SILS'_F2 and SILS'_G3 in Ref. [29]) they chose have similar molecular and interaction parameters under which Fig. 3 is obtained, that is, the samples have almost equal volume fractions of the end blocks PS and equal volume fractions of the middle blocks PI and PLA, and the incompatibility between PI and PLA is strong. Because both the PI and PLA domains cannot be differentiated in a single image in their experiment due to the limitation of staining technique, the nature of the interface between different components is unclear, meaning that the final morphologies observed in experiments cannot be clarified. Since the total volume fraction of the end blocks PS is very large and both PI and PLA form discontinuous domains, we infer according to Fig. 3 that the morphologies observed by Radlauer *et al*. in experiment are most probably HL-I phase or HJ phase. Final determination of the structures needs further experimental investigation. It is worth mentioning that although our simulations still cannot determine which morphologies were observed by Radlauer *et al*., at least the phase diagram shown in Fig. 3 can provide some clue for final structure identification.

Self-assembly Behavior under Weak Interaction between Middle Blocks B and C

In this section, we studied the self-assembly behavior in the case of weak interaction between middle blocks B and C (*i.e.*, $\chi_{BC}N = 30$). The simulation results are given in Fig. 4 in the form of phase diagram.

https://doi.org/10.1007/s10118-018-2106-y

Compared to the phase diagram shown in Fig. 3, we can see that the BC-phase-separated region shown in Fig. 4 is reduced significantly at larger f_A. When the values of $\chi_{AB}N$ and f_A are both very small, a small phase region representing di-LAM structure still exists, which is similar to the case shown in Fig. 3. An obvious difference between Fig. 3 and Fig. 4 is that most of the LAM+BD-I phase region shown in Fig. 3 is replaced by the LAM+BD-II phase, leaving only a small phase region for the LAM+BD-I phase at lower $\chi_{AB}N$ and small f_A. Moreover, two kinds of stable structures, which are not observed in the above section, are found in the region of $\chi_{AB}N < 35$ and $f_A = 0.35$, as shown in Fig. 4. One of the two structures is hexagonal honeycomb-like structure (HHL in Fig. 2g), and the other one is a new hierarchical lamella phase (HL-II in Fig. 2h), which is structurally quite similar to the HL-I structure shown in Fig. 2(d). The HHL structure is a kind of polygonal tiling structure that has already been extensively studied in star ABC triblock copolymers. This structure has been predicted by Drolet *et al*. in linear ABCA tetrablock copolymer using SCFT simulation[36, 37]. Our simulation work further demonstrates that the stable HHL phase region is quite limited compared to the overall phase-separated region shown in Fig. 4. For the HL-II structure (Fig. 2h), we can see that its structure characteristic is the same as that of the HL-I structure (Fig. 2d), except that the continuous lamella phase is constructed by one of the middle blocks (*e.g.*, block C as shown in Fig. 2h), but not by end blocks A. Although the hierarchical lamella structures shown in Figs. 2(d) and 2(h) are identical, it can be expected that they have different chain packing modes, which is schematically shown in Fig. 5. The difference in chain packing modes implies that the HL-I structure may have some, *e.g.*, mechanical, properties that are different from those the HL-II structure has.

Similar to the case shown in Fig. 3, when the chain length ratio of block A is $f_A > 0.4$, we can still obtain a relatively large phase region representing the HL-I phase in Fig. 4. However, different from the case shown in Fig. 3, the HJ phase is not obtained on the right side of the HL-I region. When the interaction parameter $\chi_{AB}N$ is increased up to 50,

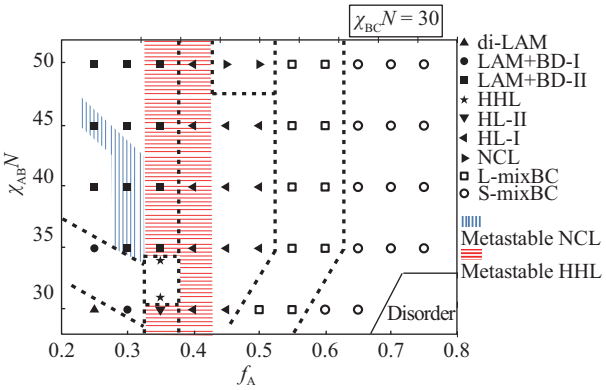

Fig. 4 Phase diagram as a function of chain length ratio of block A f_A and interaction parameter between blocks A and B $\chi_{AB}N$ at $\chi_{BC}N = 30$ (The dashed lines are used to approximately distinguish phase regions for various stable structures. Mesh grids represent regions for typical metastable structures.)

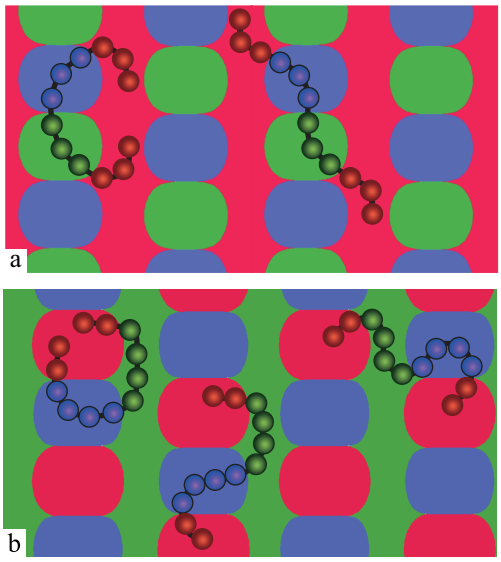

Fig. 5 Schematic representation of chain packing mode in (a) HL-I and (b) HL-II structures, respectively

another kind of noncentrosymmetric structure (*i.e.*, noncentrosymmetric lamella phase denoted by NCL in Fig. 2i) is obtained in the range of $f_A \approx 0.45-0.50$, which is shown in Fig. 4. In NCL structure, the repeating sequence of different phase domains is –A–B–C–A–B–C–, which is different from the repeating sequence of centrosymmetric lamella phase, *i.e.*, –A–B–C–B–A–. The NCL structure has some "polarizability" due to its one-way alignment of the ABCA molecules in structures, hence has many potential applications in fields such as piezoelectric and ferroelectric materials[30]. When f_A is further increased, blocks B and C do not phase separate from each other any more due to the weak interaction between them, forming a lamella phase with mixed B and C (L-mixBC in Fig. 2j). When f_A is very large (> 0.60), the S-mixBC structure is obtained again.

Another interesting phenomenon is that in Fig. 4, there are five structures (LAM+BD-I, HL-I, HHL, L-mixBC and S-mixBC) that have been observed in star ABC triblock copolymer system and only two structures (LAM+BD-I and S-mixBC) that have been observed in linear ABC triblock copolymer system[10, 14]. By comparing the transition sequence of the structures self-assembled by the ABCA tetrablock copolymers with that of star ABC system, it can be found that the transition sequence of the self-assembled structures of the ABCA system with increasing f_A is, to some extent, similar to that of star ABC system under certain interaction conditions[14]. For instance, when $\chi_{AB}N = 33$, a transition sequence of the structures, *i.e.*, HHL → HL-I → L-mixBC → S-mixBC, can be seen in Fig. 4. A generally similar transition sequence (neglecting structures that are not observed in the ABCA system) can also be seen in the star ABC system at similar interaction parameters (see Fig. 2 in Ref. [14]). This means that although the topological structures of linear ABCA tetrablock copolymer and star ABC triblock copolymer are different, the phase behavior of linear ABCA tetrablock copolymer is more similar to that of star ABC triblock copolymer than that of linear ABC

https://doi.org/10.1007/s10118-018-2106-y

triblock copolymer under certain conditions.

Metastable Behavior

It is known that metastable states are ubiquitous in complex polymer systems, which generally can be used as an effective way for structure control. Therefore, understanding metastable behavior of polymeric system is of great importance for fabricating polymeric materials with desired ordered structures in practice. In Figs. 3 and 4, structures only with the lowest free energies, *i.e.*, stable structures, were considered in the construction of the phase diagrams. In fact, many structures with higher free energies (*i.e.*, metastable states) have been found at a given condition during our simulations.

To provide more insight into the self-assembly behavior of the ABCA tetrablock copolymer, phase regions for metastable structures obtained at $\chi_{AB}N = 50$ and $\chi_{AB}N = 30$ are given in Figs. 3 and 4, respectively. We plotted, in various mesh grids, the regions for three typical metastable states, *i.e.*, NCL, HHL and HJ structures. We can see that the NCL structure can be found as metastable states at intermediate $\chi_{AB}N$ and small f_A, no matter the interaction between blocks B and C is strong (Fig. 3) or weak (Fig. 4). It should be noted that the NCL structure is found as stable state only when the interaction between middle blocks B and C is weak and its corresponding phase region is very limited, as shown in Fig. 4. Fig. 3 indicates that the interesting NCL structure can be obtained in a wider parameter window by properly tuning the metastable behavior of the copolymer system. Similar situation also applies to the noncentrosymmetric HJ structure (Fig. 3), *i.e.* the parameter window for the HJ phase is widened due to the existence of the metastable state. However, the simulation results show that the HJ structure, including stable and metastable, can only be observed in the case of strong interaction between blocks B and C. Besides these two noncentrosymmetric structures, Figs. 3 and 4 show that the metastable HHL structure can all be found at similar phase regions under different $\chi_{BC}N$, and the phase regions for metastable HHL structure are much larger than that for stable HHL structure shown in Fig. 4.

Finally, to further understand the metastable behavior of the ABCA tetrablock copolymer, we calculate the total free energy, the energy from entropy and the energy from enthalpy of the structures (including stable and metastable structures) at different f_A according to Eq. (1), the first line and the second line of Eq. (1), respectively. Taking the case of $\chi_{BC}N = 50$ and $\chi_{AB}N = 40$ as an example, we can see that structures obtained at fixed f_A have similar free energies (Fig. 6a), meaning that the free energies for various structures obtained at a given condition are close. Meanwhile, it can be seen that the variation tendency of the energies from entropy (Fig. 6b) with f_A is the same as that of the total free energies (Fig. 6a), meaning that entropy plays a dominant role during the structure transition with increasing f_A. However, as for various ordered structures obtained at a certain f_A, things are different. For instance, the stable LAM+BD-II structure obtained at $f_A = 0.35$ has the lowest total free energy compared to other metastable structures

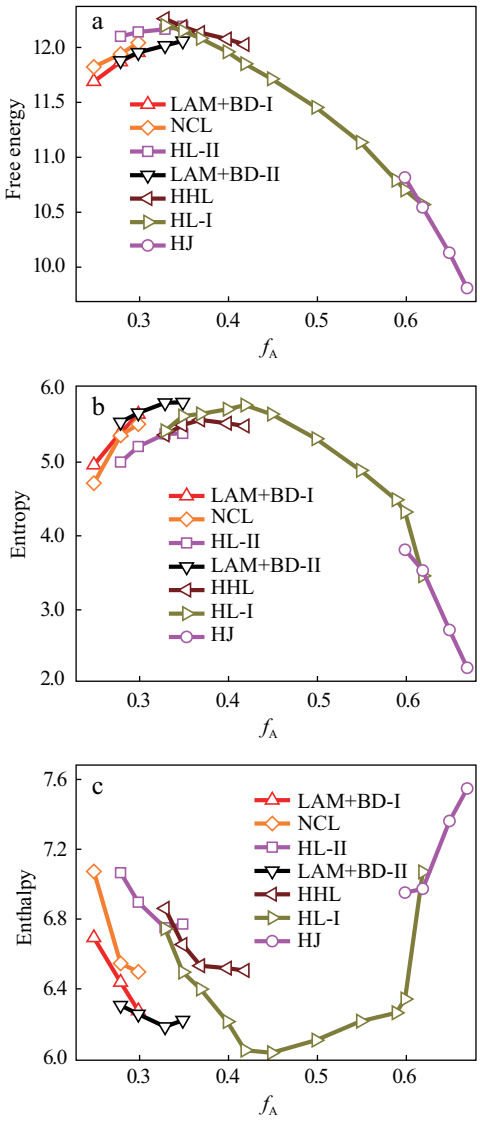

Fig. 6 (a) Total free energies, (b) energies from entropy and (c) energies from enthalpy as a function of f_A for various structures obtained at $\chi_{BC}N = 50$ and $\chi_{AB}N = 40$

obtained at the same f_A (Fig. 6a). It can be seen that the LAM+BD-II structure has the highest energy from entropy (Fig. 6b), meaning that it must have much lower energy from enthalpy (Fig. 6c) to ensure that its total free energy is the lowest. Fig. 6 indicates that enthalpy plays an important role in the metastable behavior of the ABCA tetrablock copolymer system.

CONCLUSIONS

We have systematically studied the self-assembly behavior of linear ABCA tetrablock copolymers using real-space self-consistent field theory and simulation. Ten ordered structures were obtained, including centrosymmetric diblock-like lamella phase, lamella phase with beads at interface, zigzag lamella phase with beads at interface, hierarchical lamella with continuous A phase, hierarchical lamellae with discrete A phase, hexagonal honeycomb-like phase, hexagonal

https://doi.org/10.1007/s10118-018-2106-y

spheres with mixed BC, lamella phase with mixed BC, along with noncentrosymmetric hexagonal Janus phase and lamella phase. By comparing free energies of candidate ordered structures obtained at a given condition, phase diagrams showing the effects of the chain length ratio of block A and the interaction between blocks A and B are constructed for the ABCA tetrablock copolymers with different interaction strength between blocks B and C. When the interaction strength between blocks B and C is strong, hierarchical lamella with continuous A dominates most of the phase-separated region in the phase diagram. When the interaction strength between blocks B and C becomes weak, the region of lamella phase with beads at interface is significantly reduced, leaving the zigzag lamella phase with beads at interface and the hierarchical lamella with continuous A being the dominant structures. Furthermore, the simulation results show that the stable noncentrosymmetric hexagonal Janus spheres can be observed when the interaction strength between blocks B and C is strong, whereas the stable noncentrosymmetric lamella phase can be obtained in the case of weak interaction between blocks B and C. In addition, studies on the metastable behavior of the system reveal that entropy is the main driving force for the structure transition with increasing chain length ratio of block A, while enthalpy plays an important role in the metastable behavior of the ABCA tetrablock copolymer system. The present study not only offers a new insight into the phase behavior of the linear ABCA tetrablock copolymer, but also provides a useful guide for fabricating materials with desired structures using such kind of tetrablock copolymers.

ACKNOWLEDGMENTS

This work was financially supported by the National Natural Science Foundation of China (No. 21474107). The resource provided by Computing Center of Jilin Province is gratefully acknowledged.

REFERENCES

1 Fujikawa, S.; Koizumi, M.; Taino, A.; Okamoto, K. Fabrication and unique optical properties of two-dimensional silver nanorod arrays with nanometer gaps on a silicon substrate from a self-assembled template of diblock copolymer. Langmuir 2016, 32(47), 12504−12510.
2 Higuchi, T.; Sugimori, H.; Jiang, X.; Hong, S.; Matsunaga, K.; Kaneko, T.; Abetz, V.; Takahara, A.; Jinnai, H. Morphological control of helical structures of an ABC-type triblock terpolymer by distribution control of a blending homopolymer in a block copolymer microdomain. Macromolecules 2013, 46(17), 6991−6997.
3 Nunes, S. P. Block copolymer membranes for aqueous solution applications. Macromolecules 2016, 49(8), 2905−2916.
4 Thurn-Albrecht, T.; Schotter, J.; Kastle, C. A.; Emley, N.; Shibauchi, T.; Krusin-Elbaum, L.; Guarini, K.; Black, C. T.; Tuominen, M. T.; Russell, T. P. Ultrahigh-density nanowire arrays grown in self-assembled diblock copolymer templates. Science 2000, 290(5499), 2126−2129.
5 Bates, C. M.; Maher, M. J.; Janes, D. W.; Ellison, C. J.; Willson, C. G. Block copolymer lithography. Macromolecules 2014, 47(1), 2−12.
6 Ludwigs, S.; Boker, A.; Voronov, A.; Rehse, N.; Magerle, R.; Krausch, G. Self-assembly of functional nanostructures from ABC triblock copolymers. Nat. Mater. 2003, 2(11), 744−747.
7 Ji, S. X.; Wan, L.; Liu, C. C.; Nealey, P. F. Directed self-assembly of block copolymers on chemical patterns: a platform for nanofabrication. Prog. Polym. Sci. 2016, 54-55, 76−127.
8 Matsen, M. W. Equilibrium behavior of asymmetric ABA triblock copolymer melts. J. Chem. Phys. 2000, 113(13), 5539−5544.
9 Matsen, M. W.; Schick, M. Stable and unstable phases of a diblock copolymer melt. Phys. Rev. Lett. 1994, 72(16), 2660−2663.
10 Tang, P.; Qiu, F.; Zhang, H. D.; Yang, Y. L. Morphology and phase diagram of complex block copolymers: ABC linear triblock copolymers. Phys. Rev. E 2004, 69(3), 031803.
11 Sun, M. Z.; Wang, P.; Qiu, F.; Tang, P.; Zhang, H. D.; Yang, Y. L. Morphology and phase diagram of ABC linear triblock copolymers: Parallel real-space self-consistent-field-theory simulation. Phys. Rev. E 2008, 77(1), 016701.
12 Li, W. H.; Qiu, F.; Shi, A. C. Emergence and stability of helical superstructures in ABC triblock copolymers. Macromolecules 2012, 45(1), 503−509.
13 Liu, M. J.; Li, W. H.; Qiu, F.; Shi, A. C. Theoretical study of phase behavior of frustrated ABC linear triblock copolymers. Macromolecules 2012, 45(23), 9522−9530.
14 Tang, P.; Qiu, F.; Zhang, H. D.; Yang, Y. L. Morphology and phase diagram of complex block copolymers: ABC star triblock copolymers. J. Phys. Chem. B 2004, 108(24), 8434−8438.
15 Li, W. H.; Xu, Y. C.; Zhang, G. J.; Qiu, F.; Yang, Y. L.; Shi, A. C. Real-space self-consistent mean-field theory study of ABC star triblock copolymers. J. Chem. Phys. 2010, 133(6), 064904.
16 Zhang, G. J.; Qiu, F.; Zhang, H. D.; Yang, Y. L.; Shi, A. C. SCFT study of tiling patterns in ABC star terpolymers. Macromolecules 2010, 43(6), 2981−2989.
17 Gemma, T.; Hatano, A.; Dotera, T. Monte Carlo simulations of the morphology of ABC star polymers using the diagonal bond method. Macromolecules 2002, 35(8), 3225−3237.
18 Hayashida, K.; Saito, N.; Arai, S.; Takano, A.; Tanaka, N.; Matsushita, Y. Hierarchical morphologies formed by ABC star-shaped terpolymers. Macromolecules 2007, 40(10), 3695−3699.
19 Mogi, Y.; Nomura, M.; Kotsuji, H.; Ohnishi, K.; Matsushita, Y.; Noda, I. Superlattice structures in morphologies of the ABC triblock copolymers. Macromolecules 1994, 27(23), 6755−6760.
20 Jinnai, H.; Kaneko, T.; Matsunaga, K.; Abetz, C.; Abetz, V. A double helical structure formed from an amorphous, achiral ABC triblock terpolymer. Soft Matter 2009, 5(10), 2042−2046.
21 Huang, H. L.; Yi, G. B.; Zu, X. H.; Zhong, B. B.; Luo, H. S. Patterning of triblock copolymer film and its application for surface-enhanced Raman scattering. Chinese J. Polym. Sci. 2017, 35(5), 623−630.
22 Epps, T. H.; Cochran, E. W.; Bailey, T. S.; Waletzko, R. S.; Hardy, C. M.; Bates, F. S. Ordered network phases in linear poly(isoprene-*b*-styrene-*b*-ethylene oxide) triblock copolymers. Macromolecules 2004, 37(22), 8325−8341.
23 Bates, F. S.; Hillmyer, M. A.; Lodge, T. P.; Bates, C. M.; Delaney, K. T.; Fredrickson, G. H. Multiblock polymers: Panacea or Pandora's box? Science 2012, 336(6080), 434−440.
24 Touris, A.; Chanpuriya, S.; Hillmyer, M. A.; Bates, F. S. Synthetic strategies for the generation of ABCA' type asymmetric tetrablock terpolymers. Polym. Chem. 2014, 5(19), 5551−5559.
25 Brannan, A. K.; Bates, F. S. ABCA tetrablock copolymer vesicles. Macromolecules 2004, 37(24), 8816−8819.

26 Cui, J.; Jiang, W. Structure of ABCA tetrablock copolymer vesicles and their formation in selective solvents: a Monte Carlo study. Langmuir 2011, 27(16), 10141−10147.
27 Matsuo, Y.; Konno, R.; Ishizone, T.; Goseki, R.; Hirao, A. Precise synthesis of block polymers composed of three or more blocks by specially designed linking methodologies in conjunction with living anionic polymerization system. Polymers 2013, 5(3), 1012−1040.
28 Hoogenboom, R.; Wiesbrock, F.; Leenen, M. A. M.; Thijs, H. M. L.; Huang, H. Y.; Fustin, C. A.; Guillet, P.; Gohy, J. F.; Schubert, U. S. Synthesis and aqueous micellization of amphiphilic tetrablock ter- and quarterpoly(2-oxazoline)s. Macromolecules 2007, 40(8), 2837−2843.
29 Radlauer, M. R.; Fukuta, S.; Matta, M. E.; Hillmyer, M. A. Controlled synthesis of ABCA' tetrablock terpolymers. Polymer 2017, 124, 60−67.
30 Takano, A.; Soga, K.; Suzuki, J.; Matsushita, Y. Noncentrosymmetric structure from a tetrablock quarterpolymer of the ABCA type. Macromolecules 2003, 36(25), 9288−9291.
31 Jaffer, K. M.; Wickham, R. A.; Shi, A. C. Noncentrosymmetric lamellar phase in ABCD tetrablock copolymers. Macromolecules 2004, 37(18), 7042−7050.
32 Stoenescu, R.; Graff, A.; Meier, W. Asymmetric ABC-triblock copolymer membranes induce a directed insertion of membrane proteins. Macromol. Biosci. 2004, 4(10), 930−935.
33 Jiang, W. B.; Ji, Y. Y.; Lang, W. C.; Li, S. B.; Wang, X. H. Surface-induced morphologies of ABC star triblock copolymer in spherical cavities. Chinese J. Polym. Sci. 2015, 33(11), 1503−1515.
34 Fan, J. J.; Han, Y. Y.; Cui, J. Solvent property induced morphological changes of ABA amphiphilic triblock copolymer micelles in dilute solution: a self-consistent field simulation study. Chinese J. Polym. Sci. 2014, 32(12), 1704−1713.
35 Xia, Y. D.; Chen, J. Z.; Shi, T. F.; An, L. J. Self-assembly of linear rod-coil multiblock copolymers. Chinese J. Polym. Sci. 2013, 31(9), 1242−1249.
36 Drolet, F.; Fredrickson, G. H. Combinatorial screening of complex block copolymer assembly with self-consistent field theory. Phys. Rev. Lett. 1999, 83(21), 4317−4320.
37 Drolet, F.; Fredrickson, G. H. Optimizing chain bridging in complex block copolymers. Macromolecules 2001, 34(15), 5317−5324.
38 Press W. H.; Flannery, B. P; Teukolsky, S. A.; Vettering, W. T. Numerical recipes. Cambridge Univeristy Press, Cambridge, England. 1989.
39 He, X. H.; Liang, H. J.; Huang, L.; Pan, C. Y. Complex microstructures of Amphiphilic diblock copolymer in dilute solution. J. Phys. Chem. B 2004, 108(5), 1731−1735.

https://doi.org/10.1007/s10118-018-2106-y